442 *Macromolecules* **2010**, *43*, 442–447
DOI: 10.1021/ma901947p

Macromolecules
ARTICLE

Block Copolymer−Surfactant Complexes in Thin Films for Multiple Usages from Hierarchical Structure to Nano-Objects

Jin Wook Lee, Chansub Lee, Su Yeon Choi, and Seung Hyun Kim*

Division of Nano-Systems Engineering, Inha University, Incheon 402-751, South Korea

Received September 2, 2009; Revised Manuscript Received October 29, 2009

ABSTRACT: Thin films of block copolymer−surfactant complexes which consist of polystyrene-*b*-poly(ethylene oxide) (PS-*b*-PEO) with dodecylbenzenesulfonic acid (DBSA) hydrogen-bonded to the ether group in PEO blocks, are investigated and characterized by FT-IR, DSC, AFM, TEM, GISAXS, and GIWAXD. The films are solvent-annealed for obtaining controlled orientation and high degree of lateral order of the microdomains. Selective loading of low-mass surfactant into PEO domains leads to morphological transition over wide range of phase diagram in self-assembled nanostructure of block copolymer. In addition, the self-assembly of amphiphilic surfactants combined with block copolymer produces hierarchical structure with multiple length scales and different orientations in thin films. Elimination of surfactants from the complexes by selective solvent, on the other hand, produces various nanostructured materials depending on the amount of surfactants added and microdomain orientation in thin films. Consequently, low-mass amphiphilic surfactants complexed with one component of block copolymer were shown to play multiple roles ranging from generation of hierarchical structures to production of nanoporous films and nano-objects through self-assembly and resultant phase behaviors.

Introduction

Extensive demands for smaller components in modern devices require continuous development in the area of micro- and nanofabrication. Existing methods and processes are rapidly approaching technical limit with increased production cost, which means that new nanofabrication method with much better efficiency and less cost should be developed in the near future. Among several possible alternatives, self-assembly has been recently recognized as a promising candidate for nanofabrication due to the ease and simplicity in accessing complex structures on the nanometer scale and to the diversity of structure emerging through it.[1−6]

Block copolymers are one class of such self-assembling materials, exhibiting various nanostructures via microphase-separation that is caused by the immiscibility and connectivity of the components. The interaction and composition between components in addition to molecular weight are key parameters in determining the morphology type and feature size. Even the simplest diblock copolymers can generate various well-defined, well-ordered domains ranging from spheres to cylinders to lamellae depending on the relative amount of the components, while their feature size can be controlled from ten to hundred nanometers by the molecular weight of copolymer and the strength of segmental interactions between the components. Moreover, the chemical and physical contrasts between constituent components in block copolymers provide an opportunity to fully utilize the nanostructured patterns generated by self-assembly. Therefore, block copolymers with regular nanoscopic patterns and functionality have recently attracted much attention as a strong alternative that can be used as templates and scaffolds for nanofabrication.[7−18]

*Corresponding author. Telephone: +82-32-860-7493. Fax: +82-32-873-0181. E-mail: shk@inha.ac.kr.

Utilization of block copolymer self-assembly in real applications sometimes requires more complicated structure including aperiodic patterns. Combining with supramolecular chemistry is one of strategies to obtain self-assembled structure with higher complexity since, upon using additional units of different natures and sizes, the self-assembly can effectively be tuned into hierarchical organization. Supramolecular systems containing block copolymers, which were pioneered and developed by Ikkala and ten Brinke, readily use ionic interaction, hydrogen bonding, or coordination interaction to combine block copolymer self-assembly with molecular assembly, leading to hierarchical structures having so-called "structure-within-structure" morphology with two different length scales.[19−25] On the other hand, addition of low-molar-mass supramolecules into block copolymer microdomains allows reversible change in morphology and its characteristic size through selective interaction with one component of block copolymer. Additional advantage of the block copolymer-based supramolecular systems is that they can provide a simple route to prepare nanoporous structures simply by removing low-molar-mass additives.[26−28] Remaining block copolymer supports the resultant nanoporous structure with the pore size and topology corresponding to the patterns of their parent supramolecular systems. Tremendous progresses and a number of results on generation of nanoporous structures have been presented since they can find various applications in such as gas storage, catalysis, separation, purification, templating, and fuel cell technology. Such activity has been recently expanded to the block copolymer-based supramolecular systems in thin film, and there have been presented quite a few reports on thin-film behaviors of these systems.[28−32] Generally, in thin films are involved additional issues into parameter space in determining the structure of self-assembled block copolymer due to the presence of two interfaces, polymer/substrate and polymer/air interfaces. They lead to different behaviors in thin film from in the bulk, and put more limitations on our ability that can control the self-assembly of block copolymers in a thin-film geometry. This

 Published on Web 12/07/2009

difficulty sometimes forces us to use additional external fields for controlling thin film morphology including positional and orientational orders.

In this work, the hierarchical assembly of block copolymer-based supramolecules in thin films was investigated using polystyrene-*block*-poly(ethylene oxide) (PS-*b*-PEO) and dodecylbenzenesulfonic acid (DBSA) systems where DBSA would be expected to hydrogen-bond with PEO block. Solvent annealing was applied as an external field to control the resulting nanostructure of block copolymer-based supramolecules in films since it was shown to afford controlling the orientation and degree of lateral order of periodic nanopatterns over large area.[33,34] Here, changes in morphology and characteristic size were thoroughly examined upon adding DBSA. Unprecedented morphological changes covering wide range of phase diagram were found in this work with the amount of DBSA changing. Furthermore, removing DBSA from thin films produces not only nanoporous materials but also individual nano-objects with various shapes and sizes including nanocylinders and nanospheres.

Experimental Section

Materials. Three poly(styrene-*b*-ethylene oxide) (PS-*b*-PEO) diblock copolymers with different molecular weights and compositions were purchased from Polymer Source, Inc. They are denoted as PS-*b*-PEO_L (M_{PS} = 9.5 kg/mol and M_{PEO} = 8.0 kg/mol), PS-*b*-PEO_C (M_{PS} = 20 kg/mol and M_{PEO} = 6.5 kg/mol), and PS-*b*-PEO_S (M_{PS} = 8.2 kg/mol and M_{PEO} = 1.2 kg/mol), respectively, producing lamellae, cylinders, and spheres composed of PEO blocks in bulk. Dodecylbenzenesulfonic acid (DBSA) as an amphiphilic surfactant exhibiting the molecular assembly was supplied by TCI Chem. Inc., Japan. Benzene was used as a solvent without further purification as received.

Preparation of Block Copolymer/Surfactant Complexes. PS-*b*-PEO and DBSA were separately dissolved in benzene and then mixed together at predetermined concentration. The amount of DBSA added to block copolymer solution is expressed as a molar ratio with the oxygen in PEO, i.e., [EO]/[DBSA], based on the expectation that DBSA would be selectively complexed with PEO blocks through specific interaction with oxygen atom in ethylene oxide unit.[35,36] Thin films were deposited on a silicon wafer by spin-coating. Before using, silicon substrates with a native oxide layer on the surface were cleaned by immersion in a piranha solution at 80 °C for 20 min, rinsed with Millipore water, dried under nitrogen gas. The film thickness was set to between 40 and 200 nm by controlling the spinning rate and/or solution concentration, but all the results in this work were found to be independent of the film thickness. Spin-coated films were placed in saturated benzene vapor for 6 h.

Characterization. Interaction and complex formation of DBSA with block copolymers were assessed by Fourier transform infrared (FT-IR) spectroscopy. The FT-IR spectra were recorded in transmission with a model BRUKER IFS 66v/S. Thermal behaviors of complexes were investigated by using a NETZSCH DSC200 F3 differential scanning calorimeter (DSC) under a nitrogen atmosphere. The samples were heated from 25 to 250 °C at a scan rate of 10 °C min^{-1}.

To analyze the bulk structure, both small-angle X-ray scattering (SAXS) and wide-angle X-ray diffraction (WAXD) measurements were conducted. SAXS measurements were performed on the 4C1 beamline at Pohang Accelerator Laboratory (PAL) in Korea with an X-ray wavelength of 1.608 Å. Two dimensional CCD camera (Princeton Instruments, SCX-TE/CCD-1242) was used to collect the scattered X-rays. WAXD was conducted using a Rigaku Dmax 2500 diffractometer from 2.5° to 25° at an interval of 0.05°. In order to obtain structural information on thin films, grazing-incidence small-angle X-ray scattering (GISAXS) and grazing-incidence wide-angle X-ray diffraction (GIWAXD) measurements were performed on the 4C2 beamline at Pohang Accelerator Laboratory (PAL) in Korea with a wavelength of 1.3807 Å, where the scattering patterns were taken above the critical angle of polymer films but below the critical angle of substrate.

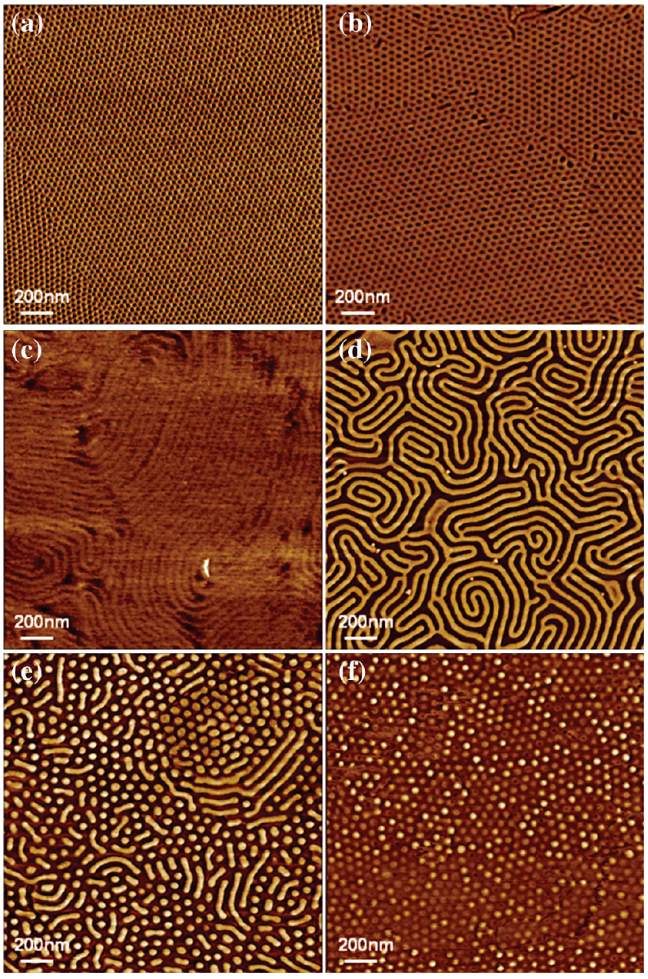

Figure 1. SFM phase images of thin films with about 50 nm thick of PS-*b*-PEO_C without DBSA (a) and of PS-*b*-PEO_C/DBSA with concentration of [EO]/[DBSA] = 32 (b), 8 (c), 2 (d), 1 (e), and 0.5 (f).

Real-space surface morphology of samples was assessed by scanning force microscopy (SFM) in both the height and phase modes using a Digital Instruments Nanoscope Multimode IVa in a tapping mode. Transmission electron microscopy (TEM) measurements were carried out on a Philips CM200 electron microscope operated at 120 kV. The TEM samples were prepared on a silicon substrate having a thick oxide layer, floated into the surface of a 5 wt % HF solution in water, transferred to a water bath, and then retrieved with a Cu grid for measurements.

Results and Discussion

Before characterizing the structure and properties of PS-*b*-PEO/DBSA complex systems, verification on the specific interaction of DBSA with block copolymer was first conducted with FT-IR and DSC measurements (see Supporting Information, Figures S1 and S2). Those results clearly indicate that the sulfonic group in DBSA interacts with the ether group in PEO blocks through hydrogen bonding.[35,36] Because of this selective interaction of DSBA with PEO blocks, the phase behavior of PS-*b*-PEO/DBSA complexes in thin film as well as in bulk is expected to depend on the concentration of DBSA added to the block copolymer. Figure 1 shows the SFM images on the film surface of complex systems between cylinder-forming PS-*b*-PEO_C

and DBSA as a function of DBSA concentration, where all samples were solvent-annealed for 6 h under benzene vapor. At low concentration of DBSA with [EO]/[DBSA] = 32 (Figure 1b), the cylindrical structure with perpendicular orientation is still generated as in case of neat PS-*b*-PEO_C without DBSA (Figure 1a) although its domain size increases. However, further increase in the DBSA concentration induces the morphological changes from cylinders at [EO]/[DBSA] = 32 through the lamellae at [EO]/[DBSA] = 8 and 2 (Figures 1c and 1d) to inverted cylinders at [EO]/[DBSA] = 1 (Figure 1e) and inverted spheres at [EO]/[DBSA] = 0.5 (Figure 1f). Such full range of phase transition has been reported previously for block copolymer system containing inorganic precursor, where block copolymer was used as a structure-directing agent for various shapes of nanoporous ceramics.[37] However, to our knowledge, there have been no reports on the morphological changes covering the whole range of phases in phase diagram by the addition of low-molar-mass supramolecules. In the most previous studies on bulk systems of block copolymer−amphiphile complexes, small range of phase transition has been reported by selectively loading amphiphiles into one particular domain, e.g. only from cylindrical to lamellar structure or vice versa in PS-*b*-P4VP/PDP systems.[20,32] In the work by Ikkala and ten Brinke, the morphological changes ranging from the spherical to inverted spherical structure for PS-*b*-P4VP/PDP system were presented together with the morphology diagram, but in that case, several PS-*b*-P4VP block copolymers with different molecular weights and compositions were used to cover the whole range of phase diagram, in contrast to our result where only one kind of block copolymer was used.[38] Similar trends were observed in thin films, and even solvent-annealed thin films of PS-*b*-P4VP/PDP exhibited the switch between only two different morphologies depending on the solvent vapor pressure.[39] On the other hand, in some other case, no morphological change was observed in thin film in spite of high concentration of amphiphilic surfactants due to the solvent selectivity.[28] Swelling of domain by the preferential solvent offsets the increase in the volume fraction of other domain by the amphiphiles selectively loaded to force the phase unchanged.[28] In our case, however, thin films of PS-*b*-PEO/DBSA complexes exhibit a wide range of transition, as shown in Figure 1. That is due to the fact that PEO blocks can interact with much more amphiphilic surfactants at comparable molecular weight because of higher number of ethylene oxide unit in one chain, which leads to an increase in the volume fraction of the (PEO + DBSA) phase. In fact, the concentration of [EO]/[DBSA] = 1 corresponds to the volume fraction of the (PEO + DBSA) phase of 0.70, which means that this complex system reaches into the cylindrical region of the phase diagram, and should exhibit the cylindrical structure of PS in the (PEO + DBSA) matrix, as shown in Figure 1e.

This morphological transition in thin films was confirmed by X-ray scattering experiments where the phase and its spatial arrangement were identified by GISAXS measurements, as shown in Figure 2. For comparison, conventional SAXS data for the bulk systems are also included. Hexagonal packing of cylinders and alternation of lamellae in complexes were confirmed through in-plane profile in GISAXS for thin films and circularly integrated pattern in SAXS for the bulks, as shown in the insets of each figure. Moreover, strong streaks in both 2D-GISAXS patterns indicate that the cylinders and lamellae are respectively oriented normal to the surface in thin films. The phase transition was found to take place at the same concentration of DBSA for both thin films and bulks. In addition, morphological change is accompanied by the variation in the characteristic size of phase-separated microdomains of which results are included in Table 1. As expected, the characteristic size of microphase-separated domains increases with DBSA added

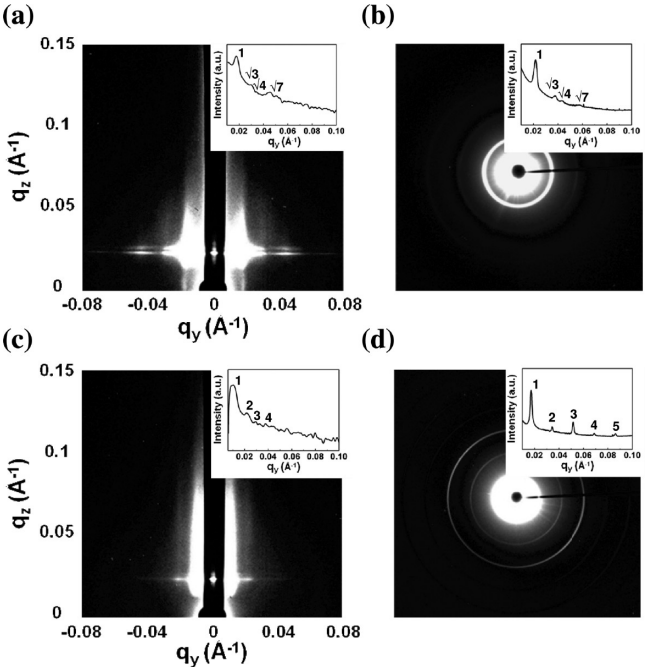

Figure 2. (a, c) GISAXS and (b, d) SAXS patterns of PS-*b*-PEO_C/DBSA with [EO]/[DBSA] = 32 (a, b) and 2 (c, d). The insets correspond to in-plane and circularly integrated profiles obtained from GISAXS and SAXS patterns, respectively.

Table 1. Domain Spacing in PS-*b*-PEO_C/DBSA Complex Systems with Different Concentration of DBSA Measured by Three Different Methods

[EO]/[DBSA]	SAXS[a] (nm)	GISAXS[b] (nm)	SFM[c] (nm)	morphology
∞	30.6	35.5	36.5	cylinder
32	33.4	41.3	41.4	cylinder
16	41.5	44.2	42.9	cylinder
8	35.4	n/a[d]	n/a[d]	lamella
4	36.5	n/a[d]	n/a[d]	lamella
2	n/a[d]	62.2	62.6	lamella
1	68.1	74.5	74.9	inverted cylinder
0.5	n/a[d]	62.9	62.7	inverted sphere

[a] Measured by small-angle X-ray scattering. [b] Measured by grazing-incidence small-angle X-ray scattering. [c] Measured by scanning force microscopy. [d] not available.

selectively into PEO domains, although discontinuity is observed as the morphological transition takes place. Then abrupt change is observed when the phase is inverted and the PS blocks become a minor component. Therefore, selective addition of amphiphiles into block copolymer domains allows forming various phases with controllable size simply by using only one kind of block copolymer in thin film as well as in bulk. The size in thin film obtained from SFM images and GISAXS data is slightly larger than that in bulk, which is due to the swelling of thin film during solvent annealing. This result indicates that solvent-annealed films may have kinetically trapping morphology, suggesting that the kinetic factors such as solvent evaporation rate and solvent vapor pressure should be carefully considered during solvent annealing.

Solvent annealing, in addition to improvement of the lateral order, can control the orientation of microdomains in PS-*b*-PEO/DBSA complexes, as in the case of neat PS-*b*-PEO block copolymer thin films. As seen in Figure 3, both orientations of cylindrical microdomains, parallel and perpendicular to the film surface, are possible through solvent annealing, irrespective of the presence of DBSA within the films. The relative humidity within

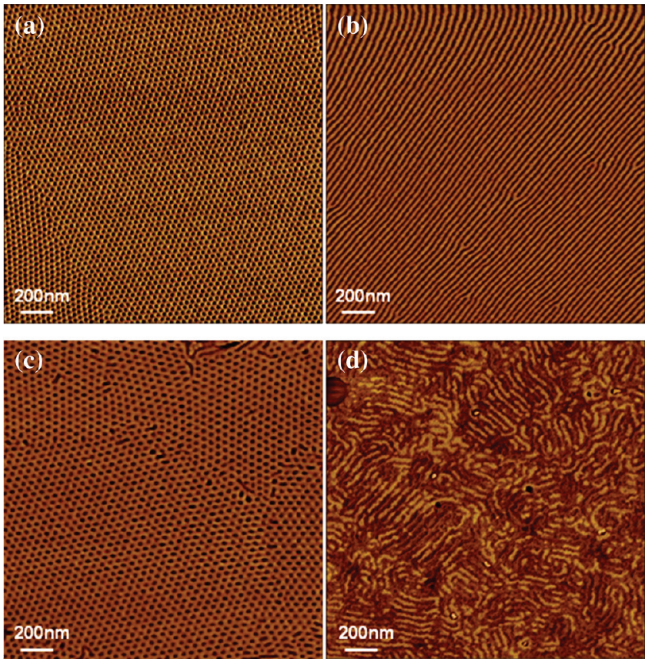

Figure 3. SFM phase images of PS-*b*-PEO_C thin films without (a, b) and with (c, d) DBSA. All films were annealed under benzene vapor for 6 h at high (a, c) and low (b, d) RH.

the chamber during the solvent annealing is a key parameter in controlling the microdomain orientation since it can control the interfacial interaction of block copolymer with solvent vapor.[40] Generally, at high RH, the interfacial interactions of block components with solvent vapor are balanced to generate the perpendicular orientation since no preferential wetting of one component exists in such case. On the other hand, at low RH is produced the parallel orientation in which case the balance of the interfacial interactions between components comprising block copolymer with the vapor is broken. Resulting preferential interaction forces the copolymer microdomains to be oriented parallel to the surface. Combined with the results in Figure 1, it is shown that the orientation and degree of lateral order can be controlled and improved by solvent annealing even for block copolymer−amphiphile complexes.

Addition of low-mass amphiphilic surfactants involves the formation of another self-assembled structure within block copolymer nanostructure, leading to a complex hierarchical structure with two different length scales. The structure on smaller length scale could not be directly observed by SFM. Instead, WAXD and GIWAXD experiments were conducted for bulk sample and thin film, respectively, and the results for PS-*b*-PEO_C/DBSA with [EO]/[DBSA] = 1 only are displayed in Figure 4. This complex has PS cylinders in (PEO+DBSA) matrix. As shown in Figure 4a, there is a diffraction peak around $2\theta \sim 3.3°$ in WAXD profile for bulk sample, which indicates the formation of self-assembled nanostructure with the characteristic length of 2.67 nm. For comparison, the WAXD profile after removing DBSA from the complex by using a selective solvent is also included in Figure 4a. Diffraction peak disappears after removing DBSA, which suggests that the nanostructure with smaller length scale is produced by the self-assembly of amphiphilic DBSA within PEO phases. In thin films, more complicated structures are observed, as seen in 2D GIWAXD pattern involving in-plane and out-of-plane profiles in Figure 4b. The out-of-plane profile, which was extracted along the q_z direction at $q_{xy} = 0$ Å^{-1}, exhibits the strong reflection peaks characteristic of the lamellar layers stacked normal to the film surface. The feature size obtained from the location of reflection

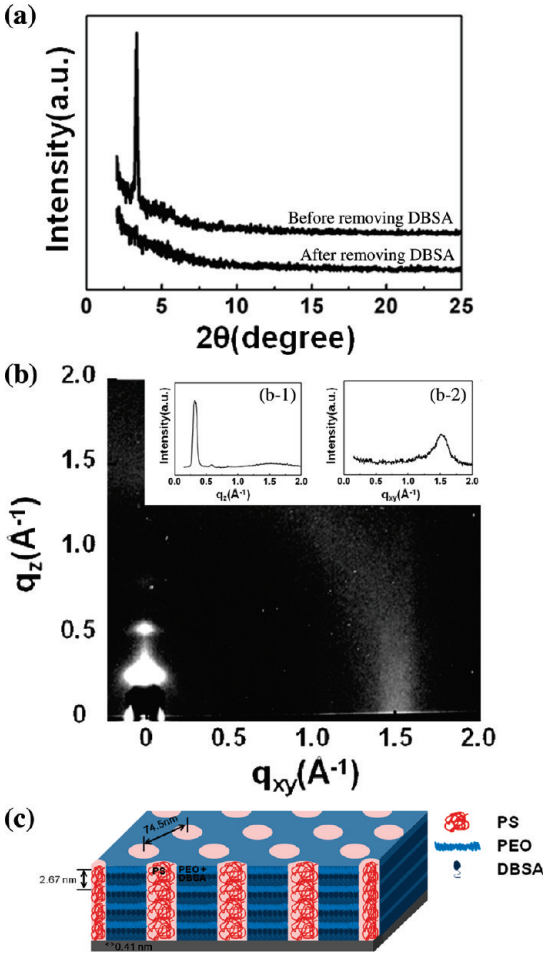

Figure 4. (a) WAXD and (b) GIWAXD patterns of PS-*b*-PEO_C/DBSA with [EO]/[DBSA] = 1 for bulk and thin film, respectively, and (c) schematic illustration of its structure in thin film. The insets in part b correspond to the out-of-plane (b-1) and in-plane (b-2) profiles obtained from the GIWAXD pattern.

peak is comparable to that from WAXD measurement. As seen in the SFM image in Figure 1e, this film has highly ordered cylindrical nanostructure where PS cylinders are oriented normal to the film plane through block copolymer self-assembly. Thus, block copolymer self-assembly guides the self-assembly of amphiphilic surfactants within PEO phases to produce highly ordered lamellar structure oriented parallel to the film plane. It should be noted that there is another weak streak at $q_{xy} = 1.5$ Å^{-1} (2θ = 19.0°) in 2D GIWAXD pattern, identified as broad scattering peak in the in-plane profile of Figure 4b. This peak may be due to the ordered bristles of DBSA that interact with the oxygen atom of the PEO blocks. The distance between the bristles is estimated at about 0.41 nm based on the peak location, which corresponds to the distance between oxygen atoms in the fully extended PEO chains when considering the bond length. These bristles are oriented normal to the film surface due to parallel stacking of lamellae in (PEO + DBSA) domains in the thin film geometry, as shown in the schematics of Figure 4c. Therefore, block copolymer self-assembly combined with amphiphilic surfactants produces hierarchically ordered nanostructure with various orientations in thin films.

Selective removal of one component from the complex system can produce various functional materials of which structures and properties can be precisely tailored in accordance with parent components and their structure. In this work, the PS-*b*-PEO/DBSA complexes were placed in water to remove low-mass DBSA without affecting the remaining structure that would be

in most part composed of hydrophobic PS. The disappearance of WAXD peak that corresponds to the lamellae-stacked structure within PEO domains after immersion in water confirms removing DBSA, as shown in Figure 4a. This leads to producing nanoporous films in the case of complexes with small amount of DBSA ([EO]/[DBSA] = 32), and the results are shown in Figure 5. Compared to the film before removing DBSA in Figure 5a, enhanced contrast in Figure 5b indicates successful extraction of DBSA, resulting in the generation of a nanoporous film with high degree of lateral order. Films with the thickness of 50 nm were attempted here for comparison by TEM before and after removing DBSA, but the results are irrespective of the film thickness. On the other hand, in the case of high content of DBSA where the (PEO + DBSA) phase constitutes the matrix, free nano-objects with various shape and size can be obtained by selectively removing DBSA. Elimination of DBSA, however, resulted in the collapse of the whole film and nanostructures so that the stable nano-object could not be obtained separately. In order to overcome this problem, the complexes were illuminated by ultraviolet radiation before the elimination of DBSA to induce the cross-linking of PS blocks, which would help to keep the original shape and obtain individual free objects. Figure 6 shows the TEM images of cross-linked PS-*b*-PEO/DBSA complexes with [EO]/[DBSA] = 0.5−2 after removal of DBSA. In all cases, (PEO + DBSA) phase corresponds to the major component, forming the matrix. The removal of DBSA from the major components forming the matrix leads to the disintegration of the film and produces isolated individual objects with nanometer scale. The shape of nano-objects obtained exactly matches the nanostructures formed by the self-assembly of block copolymer complexes in thin films. PS-*b*-PEO/DBSA with [EO]/[DBSA] = 0.5 which exhibited the spherical structure in thin film produces the nanospheres, as seen in Figure 6a. The film with [EO]/[DBSA] = 1.0 produces nanocylinders together with small population of nanospheres, as shown in Figure 6b. These nanocylinders were generated from PS-*b*-PEO/DBSA thin film with PS cylinders oriented normal to the film surface. In this case, the length of cylinders was defined by the film thickness. On the other hand, the films with parallel orientation of cylinders produced very long nanocylinders, as seen in Figure 6c. Small nano-objects observed in both cases, in addition to nanocylinders, might be generated during TEM preparation due to imperfect cross-linking of PS blocks. Similar results can be seen for PS-*b*-P4VP/PDP systems, where the nanocylinders were obtained by simply removing PDP[41] or by applying large-amplitude oscillatory shear.[42] However, in our work, the shape and size of nano-objects can effectively and precisely be controlled by changing the amount of DBSA added to the block copolymer microdomains and their orientation. Moreover, all nano-objects obtained in this work are covered by water-soluble PEO chains.

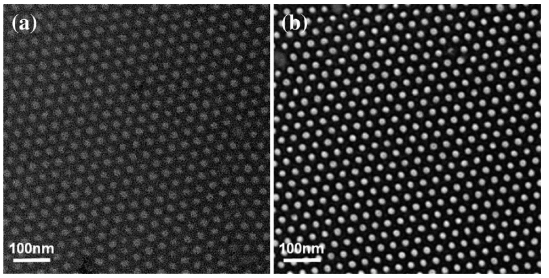

Figure 5. TEM images of PS-*b*-PEO_C/DBSA with [EO]/[DBSA] = 32 before (a) and after (b) eliminating DBSA from the complex.

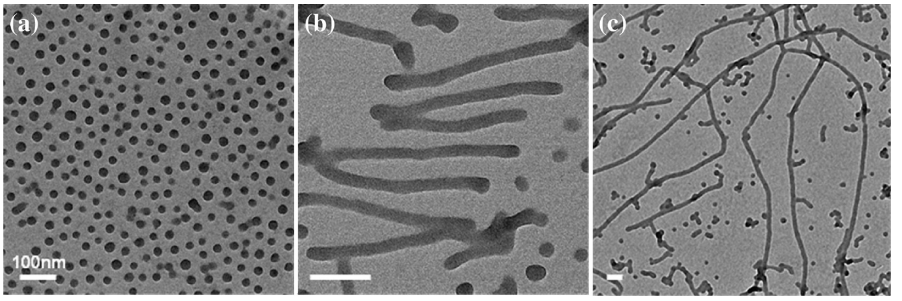

Figure 6. TEM images of PS-*b*-PEO_C/DBSA with [EO]/[DBSA] = 0.5 (a) and 1 (b, c) after eliminating DBSA from the complexes. The nano-objects in parts b and c were obtained from the films with cylinders oriented perpendicular and parallel to the surface, respectively.

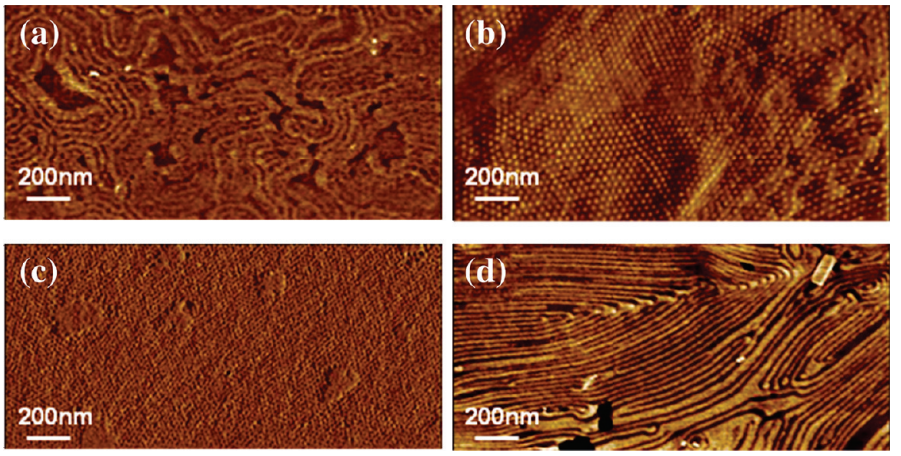

Figure 7. SFM phase images of PS-*b*-PEO_L/DBSA with [EO]/[DBSA] = 32 (a) and 2 (b) and of PS-*b*-PEO_S/DBSA with [EO]/[DBSA] = 32 (c) and 1 (d).

Similar results were obtained for other PS-*b*-PEO block copolymers with different composition and morphology, as shown in Figure 7. Lamella-forming block copolymer (PS-*b*-PEO_L) generates PS spheres in the matrix of (PEO+DBSA) on complexation with DBSA at [EO]/[DBSA] = 2, while the morphological transition from the spheres to lamellae was observed for PS-*b*-PEO_S block copolymers on complexation with DBSA at [EO]/[DBSA] = 1. In all cases, the structure-within-structure was observed, and it can also be expected that these films produce the nano-objects with the shape and size that match the structure of the PS phase in thin film after selectively removing DBSA.

Conclusions

We have demonstrated that complexation of block copolymer with low-mass self-assembling amphiphilic molecules can provide a simple route to achieving multiple goals within one system. Those include the hierarchical organization with multiple length scales, the morphological transition to new phase without synthesis of new block copolymers, and the generation of various nanostructured materials from nanoporous films to individual nano-objects. Complexation was made through simple hydrogen bonding, which allowed amphiphilic molecules to be selectively accommodated within block copolymer microdomains. Selective loading of surfactants within one particular microdomains resulted in the increase in volume fraction of that phase, which drives the complex system to cross the phase boundary to form new phase with different morphology and size. The self-assembly of amphiphilic surfactant within block copolymer led to the formation of nanostructure on the different length scales, producing elegant hierarchical structure. On the other hand, selective removal of surfactants generates the functional nanostructures with various shapes and sizes. Their shape and size could be controlled by the amount of DBSA in the complex as well as the film parameters including the film thickness and the orientation of microdomains.

This strategy is quite general and can be applied to any other block copolymer systems which can be complexed with low-mass amphiphilic surfactants. Easy incorporation of functional groups into the system allows these systems to produce well-organized, well-ordered nanostructures with specific functionality and various applications in additional to hierarchical organization.

Acknowledgment. This work was financially supported by the National Research Foundation of Korea (NRF) grant funded by the Korea government (MEST) (No. R01-2007-000-21031-0). Experiments at PLS were supported in part by MEST and POSTECH.

Supporting Information Available: Figures showing and text discussing the results of FT-IR and DSC measurements for PS-*b*-PEO/DBSA complexes. This material is available free of charge via the Internet at http://pubs.acs.org.

References and Notes

(1) Whitesides, G. M.; Grzybowski, B. *Science* **2002**, *295*, 2418–2421.
(2) Medintz, I. L.; Clapp, A. R.; Mattoussi, H.; Goldman, E. R.; Fisher, B.; Mauro, J. M. *Nat. Mater.* **2003**, *2*, 630–638.
(3) Rothemund, P. W. K. *Nature* **2006**, *440*, 297–302.
(4) Capito, R. M.; Azevedo, H. S.; Velichko, Y. S.; Mata, A.; Stupp, S. I. *Science* **2008**, *319*, 1812–1816.
(5) Douglas, S. M.; Dietz, H.; Liedl, T.; Hogberg, B.; Graf, F.; Shih, W. M. *Nature* **2009**, *459*, 414–418.
(6) Ozin, G. A.; Hou, K.; Lotsch, B. V.; Cademartiri, L.; Puzzo, D. P.; Scotognella, F.; Ghadimi, A.; Thomson, J. *Mater. Today* **2009**, *12*, 12–23.
(7) Thurn-Albrecht, T.; Schotter, J.; Kastle, G. A.; Emley, N.; Shibauchi, T.; Krusin-Elbaum, L.; Guarini, K.; Black, C. T.; Tuominen, M. T.; Russell, T. P. *Science* **2000**, *290*, 2126–2129.
(8) Cheng, J. Y.; Ross, C. A.; Chan, V. Z. H.; Thomas, E. L.; Lammertink, R. G. H.; Vancso, G. J. *Adv. Mater.* **2001**, *13*, 1174–1178.
(9) Park, M.; Chaikin, P. M.; Register, R. A.; Adamson, D. H. *Appl. Phys. Lett.* **2001**, *79*, 257–259.
(10) Lopes, W. A.; Jaeger, H. M. *Nature* **2001**, *414*, 735–738.
(11) Lazzari, M.; Lopez-Quintela, M. A. *Adv. Mater.* **2003**, *15*, 1583–1594.
(12) Hamley, I. W. *Nanotechnology* **2003**, *14*, R39–R54.
(13) Ludwigs, S.; Böker, A.; Voronov, A.; Rehse, N.; Magerle, R.; Krausch, G. *Nat. Mater.* **2003**, *2*, 744–747.
(14) Agus, H.; Wolfgang, H. B. *Small* **2006**, *2*, 600–611.
(15) Black, C. T.; Ruiz, R.; Breyta, G.; Cheng, J. Y.; Colburn, M. E.; Guarini, K. W.; Kim, H. C.; Zhang, Y. *IBM J. Res. Dev.* **2007**, *51*, 605–633.
(16) Lee, J. I.; Cho, S. H.; Park, S. M.; Kim, J. K.; Yu, J. W.; Kim, Y. C.; Russell, T. P. *Nano Lett.* **2008**, *8*, 2315–2320.
(17) Park, S. M.; Craig, G. S. W.; Liu, C. C.; La, Y. H.; Ferrier, N. J.; Nealey, P. F. *Macromolecules* **2008**, *41*, 9118–9123.
(18) Ruiz, R.; Kang, H.; Detcheverry, F. A.; Dobisz, E.; Kercher, D. S.; Albrecht, T. R.; De Pablo, J. J.; Nealey, P. F. *Science* **2008**, *321*, 936–939.
(19) Ikkala, O.; ten Brinke, G. *Science* **2002**, *295*, 2407–2409.
(20) Ikkala, O.; ten Brinke, G. *Chem. Commun.* **2004**, 2131–2137.
(21) Valkama, S.; Ruotsalainen, T.; Nykanen, A.; Laiho, A.; Kosonen, H.; ten Brinke, G.; Ikkala, O.; Ruokolainen, J. *Macromolecules* **2006**, *39*, 9327–9336.
(22) Ten Brinke, G.; Ruokolainen, J.; Ikkala, O. *Adv. Polym. Sci.* **2007**, *207*, 113−177.
(23) Takashi, K.; Norihiro, M.; Kenji, K. *Angew. Chem., Int. Ed.* **2006**, *45*, 38–68.
(24) Osuji, C. O.; Chao, C. Y.; Ober, C. K.; Thomas, E. L. *Macromolecules* **2006**, *39*, 3114–3117.
(25) Hong, J. Y.; Hong, J. L. *J. Polym. Res.* **2004**, *11*, 89–97.
(26) Maki-Ontto, R.; De Moel, K.; De Odorico, W.; Ruokolainen, J.; Stamm, M.; Ten Brinke, G.; Ikkala, O. *Adv. Mater.* **2001**, *13*, 117–121.
(27) Fustin, C. A.; Lohmeijer, B. G. G.; Duwez, A. S.; Jonas, A. M.; Schuhert, U. S.; Gohy, J. F. *Adv. Mater.* **2005**, *17*, 1162.
(28) Laforgue, A.; Bazuin, C. G.; Prud'homme, R. E. *Macromolecules* **2006**, *39*, 6473–6482.
(29) Albrecht, K.; Mourran, A.; Zhu, X.; Markkula, T.; Groll, J.; Beginn, U.; De Jeu, W. H.; Moeller, M. *Macromolecules* **2008**, *41*, 1728–1738.
(30) Tokarev, I.; Krenek, R.; Burkov, Y.; Schmeisser, D.; Sidorenko, A.; Minko, S.; Stamm, M. *Macromolecules* **2005**, *38*, 507–516.
(31) Tung, S. H.; Kalarickal, N. C.; Mays, J. W.; Xu, T. *Macromolecules* **2008**, *41*, 6453–6462.
(32) van Zoelen, W.; Asumaa, T.; Ruokolainen, J.; Ikkala, O.; ten Brinke, G. *Macromolecules* **2008**, *41*, 3199–3208.
(33) Kim, S. H.; Misner, M. J.; Xu, T.; Kimura, M.; Russell, T. P. *Adv. Mater.* **2004**, *16*, 226.
(34) Park, S.; Kim, B.; Xu, J.; Hofmann, T.; Ocko, B. M.; Russell, T. P. *Macromolecules* **2009**, *42*, 1278–1284.
(35) Chen, H. L.; Ko, C. C.; Lin, T. L. *Langmuir* **2002**, *18*, 5619–5623.
(36) Tsao, C. S.; Chen, H. L. *Macromolecules* **2004**, *37*, 8984–8991.
(37) Simon, P. F. W.; Ulrich, R.; Spiess, H. W.; Wiesner, U. *Chem. Mater.* **2001**, *13*, 3464–3486.
(38) Ruokolaonen, J.; Saariaho, M.; Ikkala, O.; ten Brinke, G.; Thomas, E. L.; Torkkeli, M.; Serimaa, R. *Macromolecules* **1999**, *32*, 1152–1158.
(39) van Zoelen, W.; Asumaa, T.; Ruokolainen, J.; Ikkala, O.; ten Brinke, G. *Macromolecules* **2008**, *41*, 3199–3208.
(40) Kim, S. H.; Misner, M. J.; Russell, T. P. *Adv. Mater.* **2008**, *20*, 4851–4856.
(41) de Moel, K.; Alberda van Ekenstein, G. O. R.; Nijland, H.; Polushkin, E.; ten Brinke, G. *Chem. Mater.* **2001**, *13*, 4580–4583.
(42) Alberda van Ekenstein, G. O. R.; Polushkin, E.; Nijland, H.; Ikkala, O.; ten Brinke, G. *Macromolecules* **2003**, *36*, 3684–3688.